Environmental Earth Sciences (2019) 78:350
https://doi.org/10.1007/s12665-019-8346-5

ORIGINAL ARTICLE

Predictive models to estimate sediment volumes deposited by debris flows (Vargas state, Venezuela): an adjustment of multivariate statistical techniques

Williams Méndez[1,2] · José Córdova[3] · Lelys Bravo de Guenni[4] · Henry Pacheco[5] · Kervin Chunga[1] · Theofilos Toulkeridis[6]

Received: 15 January 2018 / Accepted: 24 May 2019 / Published online: 6 June 2019

Abstract

Debris flows are a moving mass composed from water and solids mixture, mainly in form of sediments, with a high destructive power. The debris volume that is transported and deposited outside the drainage system of a watershed has a great importance in the definition of its hydrological response. The objective of this work was to propose predictive models generated through the adjustment of multivariate statistical techniques, to estimate the sediment volumes deposited by debris flows. Measurements and calculations of the morphometric parameters of the watersheds and drainage networks have been performed with the support of GIS software and spreadsheets. The relationships between morphometric parameters and sediment volumes have been analyzed by applying multivariate statistical techniques such as linear correlation analysis. The principal component analysis and multiple linear regression analysis have been performed with principal components, which allowed the generation of predictive models. From the predictive models generated for the sediment volumes deposited by the debris flow event of December 1999, raised results closer to reality with better Pearson's correlation coefficients from those related to the gradient and shape of the watershed relief and extension of the drainage network morphometric variables. For the estimation of deposited sediment volumes due pre- and post-1999 event conditions, only the predictive models generated with the gradient and shape of the watershed relief variable have had good results.

Keywords Morphometry · Sediment volume · Debris flow · Hydrological response · Predictive model · Multivariate statistical

Introduction

In watersheds developed in mountainous environments such as natural hydrological systems, flows are represented by volumes of water and solids that generally constitute debris as a result of rains captured in their areas of origin. These activate hydro-geomorphological processes such as erosion and runoff-related transport, which are often able to generate extreme floods and debris flows (Van Steijn 1996; Coussot and Meunier 1996; Vallance and Scott 1997; Jakob et al. 2005; Tichavský and Šilhán 2015).

These observable and measurable effects on watersheds outflows are what are known as their hydrological responses (Santi et al. 2011; Ballesteros-Cánovas et al. 2015; Palau

✉ Williams Méndez
williamsmendez@gmail.com

[1] Departamento de Construcciones Civiles, Facultad de Ciencias Matemáticas, Físicas y Químicas, Universidad Técnica de Manabí, 130105 Portoviejo, provincia de Manabí, Ecuador

[2] Centro de Investigación Estudios del Medio Físico Venezolano, Instituto Pedagógico de Caracas, Universidad Pedagógica Experimental Libertador, El Paraíso, Caracas 1020, Distrito Capital, Venezuela

[3] Departamento de Procesos y Sistemas, Universidad Simón Bolívar, Sartenejas, Baruta 1080, estado Miranda, Venezuela

[4] Departamento de Cómputo Científico y Estadística, Universidad Simón Bolívar, Sartenejas, Baruta 1080, estado Miranda, Venezuela

[5] Departamento de Ingeniería Agrícola, Facultad de Ingeniería Agrícola, Universidad Técnica de Manabí, 13132 Lodana, provincia de Manabí, Ecuador

[6] Universidad de las Fuerzas Armadas ESPE, Sangolquí, Quito, Ecuador

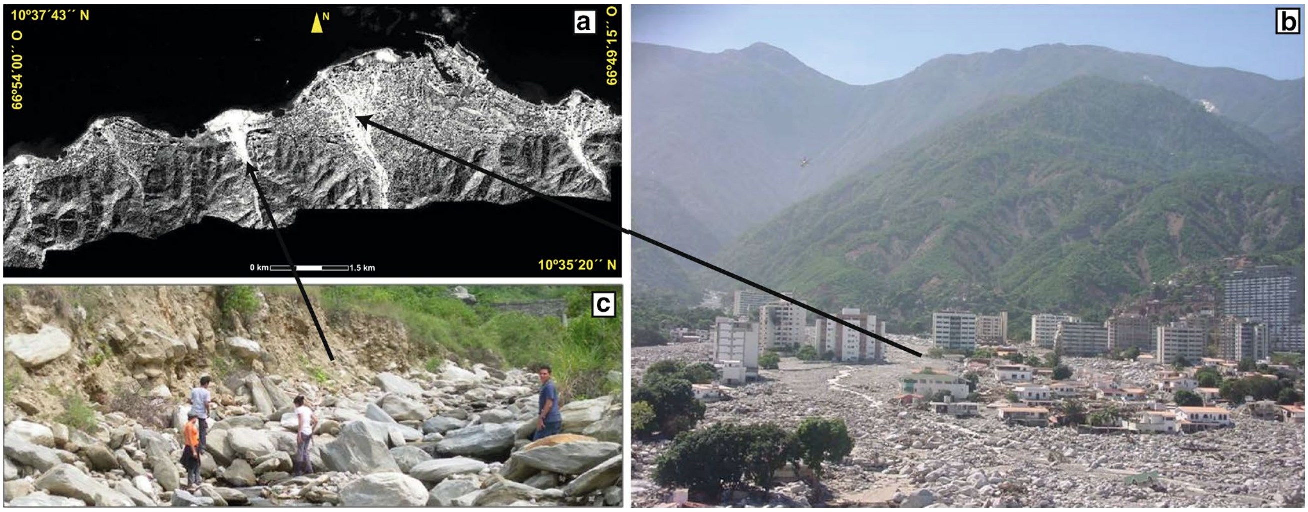

Fig. 1 Overview of deposits and effects of December 1999 debris flow event in Venezuela's Vargas state: **a** deposits (white color) of the event on the alluvial fans (from left to right) Macuto, Punta El Cojo, Camurí Chiquito, Punta El Caribe and Punta Cerro Grande, **b** impact of debris flows on the population (Los Corales sector) and **c** debris flow deposits in the main channel of the Camurí Chiquito creek (stretch over alluvial fans), dissected after the event. Satellite image IKONOS from Centro de Procesamiento Digital de Imágenes [CPDI] (1999)

et al. 2017). One of the quantifiable and important parameters in its definition, particularly in the case of debris flows, is the volume of debris that has been transported and deposited outside the watershed. In this regard, sediment volume refers to the amount of sediment, debris or solid charge present in a stream (Costa 1984, 1988; Iverson 1997). The sediment load of a debris flow is deposited due to a sudden decrease of the channel slope. This occurs when the debris flow leaves the mountainous sector and enters in a topographically flatter area. In many cases, these flat areas are alluvial fans, whose genesis is linked to the occurrence of these same hydro-geomorphological processes (debris flows).

The activation of debris flows depends on several factors such as precipitation (distribution, duration, and intensity), relief, topographic slopes, drainage network, alteration and depth of the ground cover, lithology, vegetation cover, and anthropogenic interventions. Among these factors, vegetation (types of plant formations in terms of their density and coverage) and lithology play a fundamental role in the genesis of debris flows, which has been widely demonstrated in the literature and in various localities worldwide. However, the purpose of this study is not to demonstrate that this is the case, but rather to focus on other elements of the system (morphometry of the watersheds and their drainage systems) for which little documentation has been provided on their relationship with the volumes and/or magnitudes of the deposits by debris flows.

On the other hand, the surface and vertical distribution of the different vegetal formations present in the study area, from the coastline to the summit of the studied mountain front, presents a fairly similar pattern in all watersheds. Likewise, lithological types, in which most superficially exposed rocks are foliated metamorphic, with some slight changes.

The type, structure and nature of the rocky outcrops, are determinants for the sediment granulometry generated by the action of meteorological and erosive processes, but there are also other variables that operate spatially at greater scales, such as for example, the morphometry of watersheds and their drainage systems, which ultimately determines the volumes of sediments that a watershed as a whole can contribute to a debris flow event.

The results obtained from the multivariate statistical analyzes and the models generated in this research, document interesting findings. It is demonstrated which are the specific morphometric parameter groups that have a significant relationship with the volumes of sediments of the debris flows.

The study area was chosen to be the watersheds of the north slope of the El Ávila massif, in the Vargas state, Venezuela, for the development and application of predictive models of sediment volumes. This site has been located on a relatively rugged mountainous slope, which is suitable for a torrential character with sudden and aggressive hydrological reactions, as evidenced by the sudden floods and debris flows that occurred in December 1999 (Larsen et al. 2001a, b; Pérez 2001; García-Martínez and López 2005; Nadim et al. 2006) (Fig. 1).

A series of studies have been conducted to estimate the volumes of sediments produced in watersheds, transported and deposited by rivers of the northern slope of the El Ávila massif, using a variety of other methodologies (Córdova and González 2003; Artigas et al. 2004, 2006; Hernández

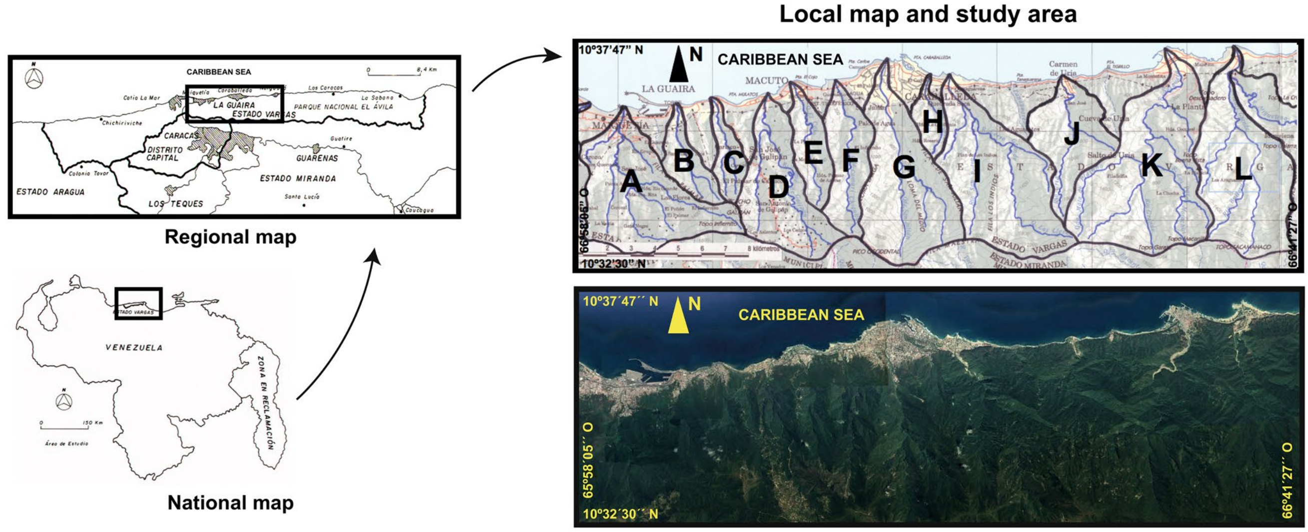

Fig. 2 Location of the watersheds of the study area: (*A*) Piedra Azul Creek, (*B*) Osorio Creek, (*C*) Cariaco Creek, (*D*) San José de Galipán River, (*E*) El Cojo Creek, (*F*) Camurí Chiquito Creek, (*G*) San Julián Creek, (*H*) Seca Creek, (*I*) Cerro Grande River, (*J*) Uria River, (*K*) Naiguatá River and (*L*) Camurí Grande River. Cartographic base from Instituto Geográfico de Venezuela Simón Bolívar [IGVSB] (2003); satellite image LANDSAT 7 ETM from CPDI (2002)

2006; López et al. 2006; Artigas and Córdova 2010; Martínez 2010) and more recent methods for estimating sediment volumes from debris flows and other types of mass disposal processes (Bremer and Sass 2012; Tiranti et al. 2016; Legorreta Paulín et al. 2017; Martha et al. 2017; Martin et al. 2017).

Other recent efforts in the study of the debris flows, have focused on analyzing and understanding the genesis of these flows linked to the occurrence of rainfall events, proposing models taking into account aspects such as thresholds, extreme events, rainfall intensity-duration and probabilities (Chen et al. 2016; Giannecchini et al. 2016; Marra et al. 2016; Bel et al. 2017; Destro et al. 2017; Dietrich and Krautblatter 2017; Fan et al. 2017; Ma et al. 2017; Wei et al. 2017).

The main objective of this study has been to explain the relationships between volumes of sediment deposited by water courses (debris flows) of mountainous environments and the morphometric parameters of watersheds and drainage systems that generate them, using multivariate statistical techniques. In addition, we seek to reduce the dimensionality of independent variables (morphometric parameters), to produce effective predictive models applicable to the studied watersheds as well as others located in similar physiographic contexts .

Study area

The watersheds selected for this study, due to their hydrogeomorphological interest resulting from the catastrophic event of December 1999, are located in the central-northern Region of Venezuela, more precisely in the central part of the Vargas state, and extend on the northern slope of the El Ávila massif, at its western end, occupies an area of about 198.89 km^2 (Fig. 2). This area is part of the Coastal Mountain Range, part of the Caribbean Mountainous System, in its central section. It is located in the eastern sector of the northern slope of the Serranía del Litoral. Specifically, on the El Ávila massif (Fig. 3).

The area borders the Caribbean Sea to the north, where the main water courses flow into the corresponding watersheds. To the south, it borders the watersheds of the southern slope of the El Ávila massif and the city of Caracas. To the east appear the Care and Anare river watersheds, La Cortada row and the Naranjal and La Cruz topographic summits, and to the west the Las Pailas and the Tacagua watersheds as well as the Tacagua pass.

Watersheds considered to be exorheic hydro-geomorphological systems in which three relief unit's characteristic of these systems have been distinguished: a catchment area, a main drainage channel and an alluvial fan, each with its own morphological characteristics and processes. Topographically, they are depressed morphology units more or less similar to funnels, a basic configuration that determines the torrential behavior of these systems. Hence, the topographic features (steep slopes between 15% and more than 45%; average slopes between 24.32 and 34.13%; heights between 25 and 2770 m.a.s.l.) indicate strong irregular terrain conditions, morphodynamic instability and sudden hydrological responses. Creeks and rivers in the studied area have very short watercourses (between 3.55 and 13.55 km) from their nascent to the mouth in the mountain front, along which they flowed, presenting steep slope variations, typical of

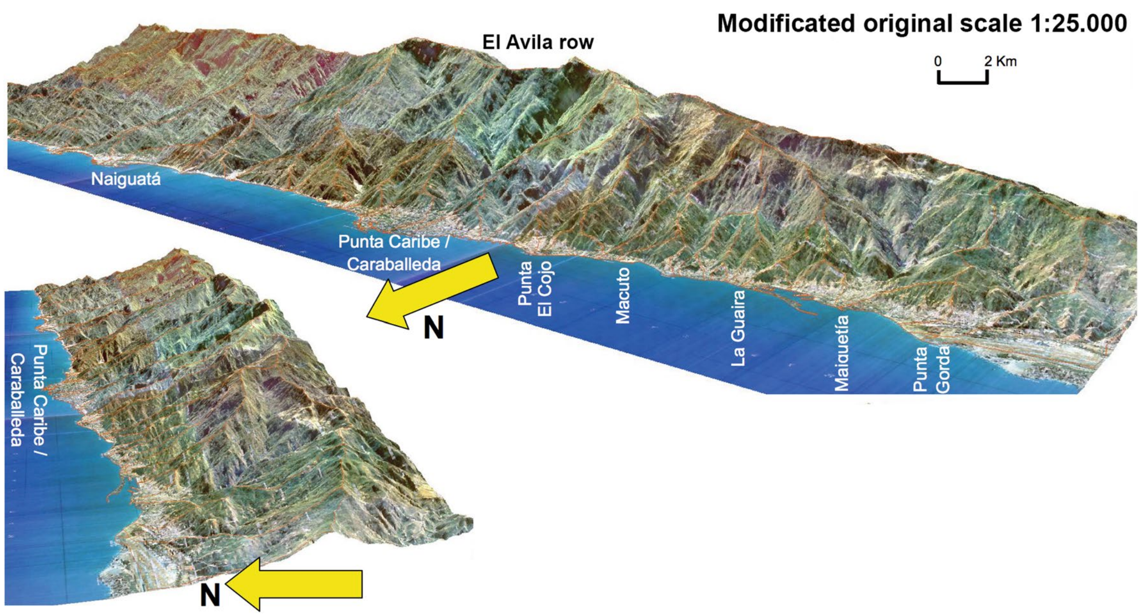

Fig. 3 3D reconstructed surface with shading overlay, on which one can appreciate the alluvial fans and watersheds of the northern slope of the El Ávila massif in the study area

torrential systems in mountainous environments with very pronounced reliefs.

Geology

The geology is represented by outcrops of lithodemic units belonging to the strips of the Ávila Metamorphic Association (Peña de Mora Augengneis, San Julián Complex, Caruao Metatonalite and Naiguatá Metagranite) and the La Costa Metamorphic Association (Serpentinite bodies, Nirgua Amphibolite, Tacagua Schist and Antímano Marble) (Urbani 1999, 2000, 2002a, b, c, d, Urbani et al. 2006). These include:

(a) *Peña de Mora Augengneis* (Paleozoic–Precambrian), with augengneises, quartzite layers, aplite dykes, marble lenses and quartz-muscovite schists.
(b) *San Julián Complex* (Paleozoic–Precambrian), with schists and quartz-plagioclase-micaceous gneisses.
(c) *Caruao Metatonalite* (Pre-Mesozoic), with meta-igneous rocks corresponding to tonalites, amphibolites, diorites, trondhjemites, granites, granodiorites, gneisses and amphibole schists.
(d) *Naiguatá Metagranite* (Pre-Mesozoic), with medium-grained leuco-syenite-granite with slight banding.
(e) *Serpentinite bodies*, including various types of serpentinites, amphibolites and rodingites.
(f) *Nirgua Amphibolite* (Mesozoic), with various types of amphibolites, schists, marbles, quartzites, gneisses, epidocites and serpentinites.
g) *Tacagua Schist* (Jurassic–Cretaceous), with dark gray and light green schists.
(h) *Antímano Marble* (Cretaceous), with massive marbles of clear gray color with layers of quartz-micaceous schists, associated with concordant bodies of amphibolic rocks.
(i) *Alluvium* (Holocene) with overlying discordance on the rocks of the La Costa Metamorphic Association in the lower parts of the watersheds. They are shaped by alluvial fans and valley bottom deposits.

Vegetation

The vegetation formations are well described in Steyermark and Huber's studies (1978), Huber and Alarcón (1988), Amend (1991) and Vareschi (1992), and for which some of their main characteristics are described below:

(a) *Littoral vegetation,* situated between sea level and 50 m.a.s.l., it is composed of very low species, mainly herbaceous, subfrutic and halophytic crawlers.
(b) *Cardonal and spine,* located between 50 and 300 m.a.s.l., is a community of low to medium size (0.5–5 m), adapted to the drought, of variable density between open to very closed, strongly armed and columnar cactus.
(c) *Deciduous forest,* low to medium height (10–20 m), with 1–2 arboreal strata and a dense understory, which is generally located between 300 and 600 m.a.s.l., has

a high percentage of deciduous tree species, and others that can reach heights between 15 and 20 m.

(d) *Semi-deciduous forest,* located between 600 and 800 m.a.s.l., of medium height and comprising 2–3 dense arboreal strata. They are composed of deciduous and evergreen trees.
(e) *Transitional forest,* located between 800 and 1500 m.a.s.l., medium to high heights (25–30 m) with 2 or 3 arboreal strata, abundant epiphytes and a relatively dense understory.
(f) *Cloudy forest,* located between 1200 and 2200 m.a.s.l., the trees are very highs and evergreen, with a great variety of epiphytic species on their trunks.
(g) *Sub-páramo,* heights higher than 2200 m.a.s.l.
(h) *Gallery forest,* they accompany the courses of rivers and creeks, the shrub and herbaceous strata are well developed.
(i) *Secondary vegetation,* atypical species of the region, the result of human intervention or reforestations.

Materials and methods

With basic cartographic information (Dirección de Cartografía Nacional [DCN], 1958, 1979; Gobernación del Distrito Federal [GDF], 1984; Servicio Autónomo de Geografía y Cartografía Nacional [SAGECAN], 1995) at scales of 1:5000 (39 topographic plans) and 1:25,000, (6 topographic charts), the base maps have been assembled with which the polygons corresponding to the study area (watersheds) have been delineated. Both map covered the entire study area. This information has been rasterized and digitized using the ArcGIS 9.2 software with its ArcHydro and Spatial Analysis modules. With this last module and using the of 1:25,000 base map, the Digital Elevation Model (DEM) of the study area was generated afterwards. Then from this, we were able to establish the longitudinal and transverse topographic profiles of the relief, as well as those of the river and creek channels.

The measurements and calculations of the morphometric parameters of the watersheds and their drainage networks were made on a digitized map at scale of 1:5000 and the DEM, obtaining basic linear, longitudinal, surface, elevation and clinometric parameters. This scale of work (1:5000) provided more accurate and approximate values for most of the basic morphometric parameters. Then, with the information obtained and the corresponding mathematical equations that define the rest of the parameters, we proceeded to their respective estimates (Table 1).

The hydrological information has been represented by the corresponding sediment volumes, namely the debris flows event of December 1999, before to the debris flows event of 1999 (Tr = 100 years) and after the debris flows event of 1999 (tr = 100 years), as previously suggested by Córdova and González (2003) and Artigas and Córdova (2010). Córdova and González (2003) had previously estimated these hydrological parameters (sediment volumes) for the same watersheds of the study area, by calibrating and applying the method developed by the U.S. Army Corps of Engineers (USACE), which takes into account the volumes of debris observed after a debris flow event, as well as a set of physical and natural variables. The volumes of debris observed were estimated by topographic–cartographic methods.

To interpret the degree of relationship between the morphometric parameters and the sediment volumes, a linear correlation analysis (LCA) has been performed. It is based on the estimation of the Pearson's correlation coefficient by the product of moments method, using the Xlstat complement of Microsoft Excel.

A principal component analysis (PCA) has been developed (Pearson 1901; Hotelling 1933) with the morphometric parameters, to reduce its dimensionality and to identify those that each has significant weight in their relationships with sediment volumes. Hereby, the type of PCA that has been performed is based on the correlations method. The PCA has been run using the SPSS Statistics Version 17.0 statistical package, for each set of parameters grouped in the same morphometric variable. The standardized scores for each watershed have been used as the values of the new variables representative of the morphometric parameters. We performed with them multiple linear regression analysis (MLRA).

The MLRA have been performed using the SPSS Statistics version 17.0 statistical package.

MLRA has been performed for each of the groups of principal components (PC), each of which represents groups of morphometric parameters as independent variables or predictors. Once the results of the MLR have been obtained, the PC's of the morphometric parameter groups that gave adequate results in their relationships with the sediment volumes have been identified, and those PC that did not satisfy the generated models have been then rejected. Predictive statistical-mathematical models have been constructed with the non-standardized coefficients (β) of the constants and the PC's generated by the MLRA. The magnitudes of the sediment volumes deposited by the main watercourses (debris flows) have been estimated according to these new models.

Results and discussion

Morphometry of watersheds and their drainage networks

Based on the morphometric parameters of the watersheds and their drainage networks (Table 2), and more particularly

Table 1 Calculated morphometric parameters for the watersheds and drainage networks

Variable	Morphometric parameter	Formula	References
Watershed scale (10 parameters)	Area (A) (km^2)	Data obtained from the GIS software	Horton (1945), Gardiner (1981)
	Larger slope area (As_{larger}) (km^2)	Data obtained from the GIS software	Horton (1945)
	Smaller slope area ($As_{smaller}$) (km^2)	Data obtained from the GIS software	Horton (1945)
	Perimeter (P) (km)	Data obtained from the GIS software	Horton (1945), Gardiner (1981)
	Length (L) (km)	Data obtained from the GIS software	Langbein (1947), Schumm (1956)
	Mean width (W_m) (km)	$W_m = A/L$	Gardiner (1981)
	Maximum width (W_{max}) (km)	Data obtained from the GIS software. It is measured perpendicular to the watershed length	Gardiner (1981)
	Diameter (D) (km)	$D = ((4A)/\pi)^{0.5}$	Gardiner (1981)
	Equivalent rectangle area to the watershed (Aer) (km^2)	$Aer = LW_{max}$	Gravelius (1914)
	Circle perimeter equal to the watershed area (Pc) (km)	$Pc = \pi((4A)/\pi)^{0.5}$	Gardiner (1981)
Gradient and shape of the watershed relief (18 parameters)	Minimum height (h) (masl)	Data obtained from the GIS software	Strahler (1952)
	Maximum height (H) (masl)	Data obtained from the GIS software	Strahler (1952)
	Mean height (H_m) (masl)	Data obtained from the GIS software	Horton (1932), Langbein (1947)
	Main stream rising height (H_r) (masl)	Data obtained from the GIS software	Strahler (1952)
	Main stream outlet height (h_o) (masl)	Data obtained from the GIS software	Strahler (1952)
	Maximum relief (R_{max}) (m)	$R_{max} = H - h$	Strahler (1952, 1957), Hadley and Schumm (1961)
	Relief ratio (R) (m/km)	$R = R_{max}/L$	Horton (1945), Schumm (1963)
	Mean relief slope (S_m) (m/m)	Data obtained from the GIS software	Horton (1932), Roche (1963), Sreedevi et al. (2005)
	Concavity of the main stream longitudinal profile (Cms)	$Cp = b/B$ $b = B - z$ where b height difference between B and z, B straight line height of the main stream longitudinal profile in its median length; and z main stream longitudinal profile height in its median length	Horton (1932), Schumm (1956)
	Mean slope of the main stream longitudinal profile (Sms_m) (m/m)	Data obtained from the main stream longitudinal profile, using Excel software	Horton (1932), Schumm (1956), Sreedevi et al. (2005)
	Main stream maximum relief (Rms_{max}) (m)	$Rms_{max} = H_r - h_o$	Strahler (1952), Hadley and Schumm (1961)
	Main stream topographic factor (Tfms)	$Tfms = Rms_{max}(Sms_m)^{0.5}$	Potter (1953)
	Mean slope of the drainage network total streams (Sts_m) (m/m)	$Sts_m = \Sigma Ss/N_t$ where Ss slope of each network stream	Horton (1932), Schumm (1956)
	Hypsometric integral (HI)	$HI = (H_m - h)/(H - h)$	Strahler (1952, 1957), Pike and Wilson (1971)
	Massiveness coefficient (Cm) (masl/km^2)	$Cm = H_m/A$	De Martonne (1909)
	Orographic coefficient (Co)	$Co = H_m Cm$	Henao (1998)
	Relative relief (Rr) (m/km)	$Rr = R_{max}/P$	Schumm (1956), Melton (1957)
	Melton roughness number (MRn)	$MRn = R_{max}A^{0.5}$	Melton (1957, 1965)

Table 1 (continued)

Variable	Morphometric parameter	Formula	References
Watershed shape (14 parameters)	Elongation (E)	$E = A^{0.5}/L$	Gardiner (1981)
	Relative crenulation perimeter (Prc)	$Prc = P^2/A$	Schumm (1956), Gardiner (1981)
	Compactness coefficient (Kc)	$Kc = 0.28(P/(A)^{0.5})$	Gravelius (1914), Horton (1945)
	Lengthening index (Il)	$Il = L/W_{max}$	Henao (1998)
	Homogeneity index (Ih)	$Ih = A/Aer$	Henao (1998)
	Symmetry index (Is)	$Is = Ah_{larger}/Ah_{smaller}$	Henao (1998)
	Form factor (Ff)	$Ff = A/L^2$	Horton (1932, 1945)
	Caquot lengthening (Cl)	$Cl = L/A^{0.5}$	–
	Elongation ratio (Re)	$Re = D/L$	Schumm (1956)
	Circularity ratio (Rc)	$Rc = (4\pi A)/P^2$	Miller (1953), Strahler (1964), Mueller (1968)
	Form index (If)	$If = P/(2\pi A)^{0.5}$	Horton (1932), Horton (1945)
	Watershed length-area index ($I_{l\text{-}a}$)	$I_{l\text{-}a} = D/A^{0.5}$	Hack (1957)
	Form coefficient (Cf)	$Cf = W_m/L$	Horton (1932, 1945)
	Roundness coefficient (Cr)	$Cr = (\pi L^2)/(4A)$	Seyhan (1977)
Extension of the drainage network (15 parameters)	Main stream length (Lms) (km)	Data obtained from the GIS software	Mueller (1968), Shreve (1974)
	Main stream valley mean length (Lv_m) (km)	Data obtained from the GIS software	Mueller (1968)
	Total length of the drainage network streams (Lts) (km)	$Lts = \Sigma Ls$ where Ls length of each drainage network stream. Data obtained from the GIS software	Horton (1945)
	Main stream total sinuosity (S)	$S = Lms/L_{min}$ L_{min} shorter distance (straight line) between the start and end of the main stream	Schumm (1977), Morisawa (1985)
	Main stream topographic sinuosity (St)	$St = Lv_m/L_{min}$	Schumm (1977), Morisawa (1985)
	Main stream hydraulic sinuosity (Sh)	$Sh = Lms/Lv_m$	Schumm (1977), Morisawa (1985)
	Main channel gravity center (Gc) (km)	It is located on the course middle of main channel. Data obtained from the GIS software	–
	Drainage density (Dd) (km/km^2)	$Dd = Lts/A$	Horton (1932, 1945)
	Drainage texture (Dt) (km^{-1})	$Dt = DdFs_m$	Smith (1950), Strahler (1952, 1957, 1964), Faniran (1968)
	Channel maintenance coefficient (Cmc) (km^2/km)	$Cmc = A/Lts$	Schumm (1956)
	Surface runoff mean extent (E_m) (km)	$E_m = A/(4Lts)$	Horton (1945)
	Surface flow length (Lsf) (km)	$Lsf = 1/((2Dd)(1-(Sts_m/S_m)^{0.5}))$	Horton (1945)
	Topographic texture (Tt)	$LogTt = 0.219649 + (1.115 \log Dd)$	–
	Drainage intensity (Di) (km)	$Di = Fs_m/Dd$	Faniran (1968)
	Mean remoteness (R_m)	$R_m = Lms/A^{0.5}$	–

Table 1 (continued)

Variable	Morphometric parameter	Formula	References
Order and magnitude of the drainage network (9 parameters)	Total number of drainage network streams (N_t)	Sum of total streams of all the orders of the drainage network	Strahler (1952, 1957, 1964)
	Watershed order (u)	Corresponds to the order number of the higher order stream segment	Strahler (1952, 1957, 1964)
	Mean bifurcation ratio (Rb_m)	It is calculated from the exponential equation obtained by plotting the streams number of a given order against the stream order	Horton (1945), Strahler (1957)
	Mean stream length ratio (Rl_m)	It is calculated from the exponential equation obtained by plotting the cumulative mean length of the streams of a given order against the stream order	Horton (1945)
	Mean slope ratio (Rs_m)	It is calculated from the exponential equation obtained by plotting the mean slope of the streams of a given order against the stream order	Horton (1945)
	Mean frequency of the drainage network total streams (Fs_m) (N_t/km^2)	$Fs_m = N_t/A$	Melton (1958), Strahler (1964)
	Torrentiality coefficient (Ct) (N_1/km^2)	$Ct = N_1/A$ where N_1 = 1st order stream total number	Melton (1958), Strahler (1964)
	Storage coefficient (Cs)	$Cs = Rl_m/Rb_m$	Horton (1945)
	Watershed magnitude (M) (N_1)	$M = N_1$	Strahler (1952, 1957, 1964)

Table 2 Morphometric parameters of the watersheds and drainage networks

Statistic	A (km^2)	As$_{larger}$ (km^2)	As$_{smaller}$ (km^2)	P (km)	L (km)	W_m (km)	W_{max} (km)	D (km)	Aer (km^2)	Pc (km)
Maximum value	31.38	25.55	8.83	25.10	8.70	3.74	6.18	6.32	51.79	19.86
Minimum value	2.89	1.63	1.26	6.80	2.88	1.00	1.40	1.92	4.03	6.03
Mean	13.89	9.23	4.65	16.15	6.08	2.06	3.26	3.97	22.05	12.46

Statistic	h (masl)	H (masl)	H_m (masl)	H_r (masl)	h_o (masl)	R_{max} (m)	R (m/km)	S_m (m/m)	Cms	Sms$_m$ (m/m)
Maximum value	125	2770	1316.76	2550	125	2745	442.50	0.34	0.71	0.41
Minimum value	25	1280	547.71	1200	25	1230	270.83	0.24	0.00	0.20
Mean	48.85	2122.08	939.70	2040.38	48.85	2073.23	353.45	0.30	0.39	0.27

Statistic	Rms$_{max}$ (m)	Tfms	Sts$_m$ (m/m)	HI	Cm (masl/km^2)	Co	Rr (m/km)	MRn	E	Prc
Maximum value	2525	1367.37	0.82	0.55	195.57	154,518.28	180.88	0.91	0.68	25.94
Minimum value	1150	666.30	0.50	0.35	34.74	36,620.01	92.20	0.42	0.48	16.00
Mean	1991.54	1020.23	0.65	0.43	98.66	84,764.85	136.94	0.63	0.57	21.38

Statistic	Kc	Il	Ih	Is	Ff	Cl	Re	Rc	If	I$_{l\text{-}a}$
Maximum value	1.43	3.01	0.77	4.38	0.46	2.08	0.76	0.79	2.03	1.13
Minimum value	1.12	1.36	0.51	1.01	0.23	1.48	0.54	0.48	1.60	1.13
Mean	1.29	2.03	0.64	1.89	0.33	1.77	0.64	0.60	1.84	1.13

Statistic	Cf	Cr	Lms (km)	Lv$_m$ (km)	Lts (km)	S	St	Sh	Gc (km)	Dd (km/km^2)
Maximum value	0.46	3.40	13.55	11.00	255.55	1.66	1.34	13.55	11.00	255.55
Minimum value	0.23	1.72	3.55	3.00	34.03	1.09	1.02	3.55	3.00	34.03
Mean	0.33	2.50	7.86	6.75	123.33	1.33	1.13	7.86	6.75	123.33

Statistic	Dt (km^{-1})	Cmc (km^2/km)	E$_m$ (km)	Lsf (km)	Tt	Di (km)	R$_m$	N_t	u	Rb$_m$
Maximum value	1136.46	0.18	0.04	0.10	1.52	5.21	2.80	1120	6	4.99
Minimum value	87.08	0.07	0.02	0.03	1.06	2.75	1.83	169	4	3.58
Mean	430.41	0.11	0.03	0.05	1.30	4.09	2.27	497.54	5.15	4.10

Statistic	Rl$_m$	Rs$_m$	Fs$_m$ (N$_t$/km^2)	Ct (N$_1$/km^2)	Cs	M (N_1)
Maximum value	2.84	1.66	76.92	60.85	0.58	886
Minimum value	1.92	1.16	15.48	11.72	0.50	127
Mean	2.26	1.41	40.83	31.51	0.55	384.54

those referred to the watershed scale variable, these hydro-geomorphological systems fall into the category of micro-watersheds due to their small dimensions. Regarding the parameters of the gradient and shape of the watershed relief variable, they are defined as topographically very rugged areas with steep slopes and large altitudinal roughness. The watershed shape parameters indicate that they are semi-circular to semi-elongated planimetric morphologies, while in the case of the extension of the drainage network parameters, they indicate branched drainage systems, and considerable densities at short lengths and small sinuosity channels being rectilinear. In the case of the order and magnitude of the drainage network variable, its parameters indicate networks of high magnitudes and orders, as well as high levels of torrentially.

The geometry of the systems (watershed scale parameters) are the ones that determine in greater proportion the specific conditions that favor the occurrence of flash floods, with hydrographs of sharp peaks and short duration. They also occur as shorter concentration times in the presence of significant storms in intensity, duration and dimensions, as they determine are the areas where rainwater is collected. In addition to the morphometric parameters grouped in the scale watershed variable, others corresponding to variables defining different attributes of these hydro-geomorphological systems, contribute in the same way to a significant weight in controlling the amplitudes and characteristics of the hydrological and morphodynamic responses of the watersheds.

These morphometric parameters are represented in specific by the slopes of the longitudinal profiles of the main creeks and rivers, the prominent mountainous relief (massiveness coefficient, orographic coefficient and Melton roughness number), the short lengths of the main

Table 3 Correlation coefficients between the sediment volumes and the morphometric parameters of the watersheds and drainage networks

Hydrological response parameter Morphometric parameter	Sediment volume (event of December 1999) (Vs-Dec1999) (m^3)	Sediment volume prior to the debris flows (Tr = 100 years) ($Vs_{prior\text{-}df}$) (m^3)	Sediment volume after the debris flows (Tr = 100 years) ($Vs_{after\text{-}df}$) (m^3)
Area (km^2)	**0.71***	**0.73**	**0.73**
Larger slope area (km^2)	0.66	**0.73**	**0.73**
Smaller slope area (km^2)	**0.70**	0.57	0.55
Perimeter (km)	0.69	**0.72**	**0.70**
Length (km)	0.66	0.66	0.63
Mean width (km)	**0.75**	**0.78**	**0.77**
Maximum width (km)	0.67	0.68	0.68
Diameter (km)	**0.74**	**0.75**	**0.74**
Equivalent rectangle area to the watershed (km^2)	0.67	0.67	0.66
Circle perimeter equal to the watershed area (km)	**0.74**	**0.75**	**0.74**
Minimum height (masl)	0.40	0.24	0.25
Maximum height (masl)	0.42	0.33	0.31
Mean height (masl)	0.48	0.42	0.40
Main stream rising height (masl)	0.34	0.30	0.29
Main stream outlet height (masl)	0.40	0.24	0.25
Maximum relief (m)	0.38	0.30	0.29
Relief ratio (m/km)	**−0.73**	**−0.80**	**−0.78**
Mean relief slope (m/m)	−0.08	−0.15	−0.16
Concavity of the main stream longitudinal profile	0.13	0.14	0.16
Mean slope of the main stream longitudinal profile (m/m)	**−0.73**	**−0.77**	**−0.75**
Main stream maximum relief (m)	0.30	0.28	0.26
Main stream topographic factor	−0.17	−0.23	−0.23
Mean slope of the drainage network total streams (m/m)	−0.19	−0.21	−0.21
Hypsometric integral	0.25	0.35	0.31
Massiveness coefficient ($masl/km^2$)	**−0.76**	**−0.75**	**−0.74**
Orographic coefficient	**−0.73**	**−0.71**	**−0.73**
Relative relief (m/km)	**−0.73**	**−0.81**	**−0.80**
Melton roughness number	**−0.80**	**−0.83**	**−0.83**
Elongation	0.68	0.69	**0.71**
Relative crenulation perimeter	−0.50	−0.37	−0.41
Compactness coefficient	−0.49	−0.35	−0.40
Lengthening index	−0.50	−0.48	−0.51
Homogeneity index	0.21	0.24	0.24
Symmetry index	0.43	0.63	0.63
Form factor	0.67	0.69	**0.72**
Caquot lengthening	−0.68	−0.67	**−0.70**
Elongation ratio	0.68	0.69	**0.71**
Circularity ratio	0.45	0.29	0.35
Form index	−0.49	−0.35	−0.40
Form coefficient	0.67	0.69	**0.72**
Roundness coefficient	−0.68	−0.66	−0.69
Main stream length (km)	0.51	0.57	0.56
Main stream valley mean length (km)	0.63	0.67	0.65

Table 3 (continued)

Hydrological response parameter Morphometric parameter	Sediment volume (event of December 1999) (Vs-Dec1999) (m^3)	Sediment volume prior to the debris flows (Tr = 100 years) ($Vs_{prior\text{-}df}$) (m^3)	Sediment volume after the debris flows (Tr = 100 years) ($Vs_{after\text{-}df}$) (m^3)
Total length of the drainage network streams (km)	0.53	0.58	0.58
Main stream total sinuosity	−0.23	−0.07	−0.06
Main stream topographic sinuosity	0.32	0.45	0.47
Main stream hydraulic sinuosity	**−0.72**	−0.61	−0.63
Main channel gravity center (km)	0.51	0.57	0.56
Drainage density (km/km^2)	−0.58	−0.52	−0.50
Drainage texture (km^{-1})	−0.46	−0.38	−0.36
Channel maintenance coefficient (km^2/km)	0.65	0.65	0.62
Surface runoff mean extent (km)	0.65	0.65	0.62
Surface flow length (km)	0.58	0.60	0.57
Topographic texture	−0.63	−0.60	−0.58
Drainage intensity (km)	−0.54	−0.52	−0.49
Mean remoteness	−0.69	−0.55	−0.58
Watershed order	0.41	0.51	0.50
Total number of drainage network streams	0.37	0.44	0.44
Mean bifurcation ratio	−0.26	−0.44	−0.42
Mean stream length ratio	−0.12	−0.29	−0.25
Mean slope ratio	0.04	−0.09	−0.07
Mean frequency of the drainage network total streams (N_t/km^2)	−0.52	−0.47	−0.44
Torrentiality coefficient (N_1/km^2)	−0.49	−0.44	−0.42
Storage coefficient	0.29	0.33	0.38
Watershed magnitude (N_1)	0.36	0.44	0.43

*Significant correlation coefficients (p value ≤ 0.05)

watercourses, the high orders of the watersheds considering that they are small systems, the total number of drainage system streams and their magnitudes.

Hydrological response: sediment volumes

The hydrological response parameters to which this study refers are fundamentally related to sediment volumes, as expressions of hydrologic dynamics that distinguish the hydro-geomorphological systems of mountainous environments and their torrential behaviors. The sediment volumes transported during the debris flows event of December 1999 ranged from 839,182 to 2,636,280 m^3, with an average of 1,685,968.42 m^3. For volumes of sediment produced under pre- and post-debris flows conditions of December 1999 and for a 100 years return period, these values ranged between 484,302 and 1,313,876.60 m^3 in the first case, and between 559,328.60 and 1,450,556.80 m^3 for the second, with average values of 867,840.55 m^3 and 1,023,799.75 m^3 respectively .

These magnitudes refer to the solid discharges in the watersheds hydrological responses, representing significant amounts that demonstrate the aggression, the hydrologic and morphodynamic power of the debris flows events that have occurred and could occur in the future in the studied sector, under the combination of triggering effects such as extraordinary rainfall and conditions of high susceptibility of the physical environment such as lithology, slope, landforms, vegetation, drainage, and soils.

Linear correlation analysis

The LCA provided a first approximation of the degree of relationship between the dependent variables (morphometric parameters) and independent variables (volumes of sediments) involved in the study and allowed us to identify the specific morphometric parameters first, that have greater significance in terms of their impact or control on the hydrological response (debris flows) of the watersheds.

Table 4 Explained total variance for the principal components of the morphometric parameters of the watersheds and drainage networks

Variable	Component	Initial eigenvalues			Extraction sums of squared loadings			Rotation sums of squared loadings		
		Total	% of variance	Cumulative %	Total	% of variance	Cumulative %	Total	% of variance	Cumulative %
Watershed scale (includes 10 morphometric parameters)	1	9.438	94.381	**94.381**	9.438	94.381	**94.381**	–	–	–
Gradient and shape of the watershed relief (includes 18 morphometric parameters)	1	7.548	41.935	41.935	7.548	41.935	41.935	6.149	34.161	34.161
	2	5.415	30.082	72.016	5.415	30.082	72.016	5.757	31.984	66.145
	3	1.971	10.952	82.969	1.971	10.952	82.969	2.274	12.636	78.781
	4	1.520	8.446	**91.415**	1.520	8.446	**91.415**	2.274	12.634	91.415
Watershed shape (includes 13 morphometric parameters)	1	9.072	69.788	69.788	9.072	69.788	69.788	7.333	56.409	56.409
	2	2.703	20.792	**90.579**	2.703	20.792	**90.579**	4.442	34.170	90.579
Extension of the drainage network (includes 15 morphometric parameters)	1	7.867	52.447	52.447	7.867	52.447	52.447	6.790	45.264	45.264
	2	4.450	29.670	82.117	4.450	29.670	82.117	4.799	31.991	77.256
	3	1.755	11.698	**93.815**	1.755	11.698	**93.815**	2.484	16.559	93.815
Order and magnitude of the drainage network (includes 9 morphometric parameters)	1	3.900	43.338	43.338	3.900	43.338	43.338	3.886	43.183	43.183
	2	2.602	28.912	72.250	2.602	28.912	72.250	2.338	25.978	69.161
	3	1.116	12.396	**84.646**	1.116	12.396	**84.646**	1.394	15.485	84.646

Bold values represent the principal component number of each variable, in which the cumulative variance (%) reaches more than 80% representativeness

The best correlation coefficients (> 0.70; *p* value ≤ 0.05) between the sediment volumes and the morphometric parameters of the watersheds and drainage networks have been observed, in order of importance for the gradient and shape of the watershed relief and watershed scale variables (Table 3). The correlation coefficients obtained with the parameters of the watershed scale variable are significant, since they have values between 0.66 and 0.78, similarly indicating a considerable weight of the watershed dimensions in the sediment yield and transport during extreme events. Morphometric parameters with the best correlations (> 0.70) with sediment volumes are the area, mean width, diameter and circle perimeter equal to the watershed area (Table 3).

The morphometric parameters of the gradient and shape of the watershed relief variable with good correlation coefficients (> 0.70; ≤ 0.05) with the sediment volumes have been those linked to inequalities (relief ratio), slopes (mean slope of the main stream longitudinal profile) and the prominent mountainous relief (massiveness coefficient, orographic coefficient, relative relief and Melton roughness number). These coefficients have been negative because the lower slopes of the main streams and a relatively less mountainous terrain correspond to watersheds of greater areas. However, the greater slopes and the more pronounced mountainous terrain present the watersheds of less extensive areas. This is the result of denudation rates (vertical and regressive erosion) of the most pronounced relief in the watersheds of larger areas.

Principal components analysis of morphometric parameters

According to the analysis of the total explained variance (ATEV) in the PCA (Table 4), all the morphometric parameters grouped in the watershed scale variable are explained in the same component (PC 1), in because of their high correlations between all these parameters. Thus, PC 1 correlates with 94.38% of the grouped parameters. In the case of the gradient and shape of the watershed relief variable, four PC have been obtained which correlate together for approximately 91.42% of the parameters representing the mentioned variable (Fig. 4). With the watershed shape variable, ATEV achieved its best percentage of representation in two PCs that total up 90.58% of the parameters that represent it. For the extension of the drainage network variable, three PCs have been generated, in the third of which 93.82% of the cumulative total variance has been correlated. Within the order and magnitude of the drainage network variable, three PCs have been obtained in the same form, in which an accumulated PC 3 explained and reached a total variance of 84.65%.

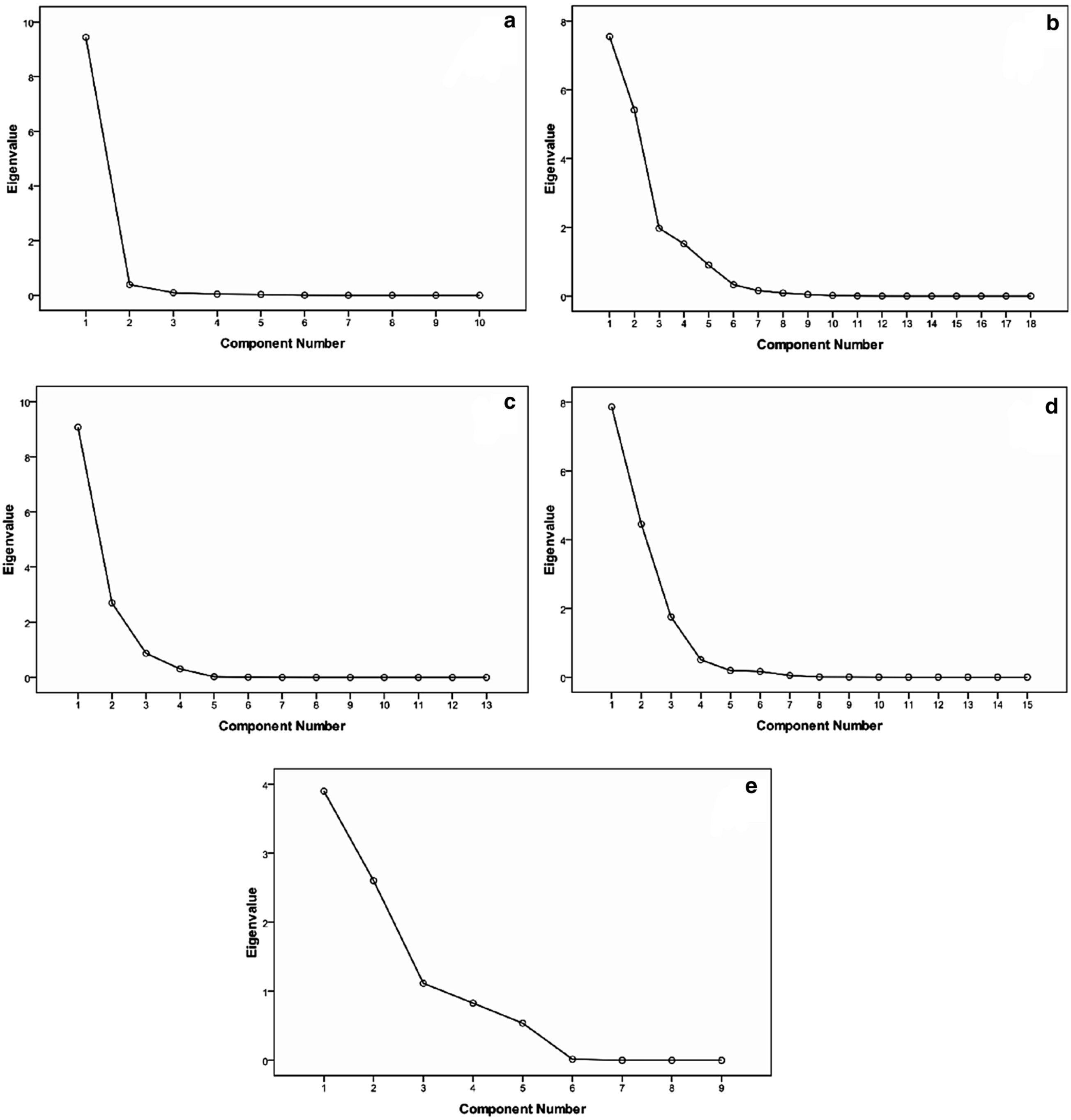

Fig. 4 PC diagrams of the morphometric parameters corresponding to the variables **a** watershed scale, **b** gradient and shape of the watershed relief, **c** watershed shape, **d** extension of the drainage network and **e** order and magnitude of the drainage network

The coefficients obtained from the scores (weights) for each parameter of each morphometric variable, which have been regrouped according to the PC (new variables), we observed that in the watershed scale variable, all its parameters have similar scores. For the other morphometric variables, significant differences have been observed regarding their score coefficients for each morphometric parameter, and according to each PC in which they have been grouped, allowed to rank them in order of importance (Fig. 5).

Multiple linear regression analysis

The models generated by the MLRA between the PC of the watershed scale variable and sediment volumes produced good correlation coefficients (between 0.730 and 0.742)

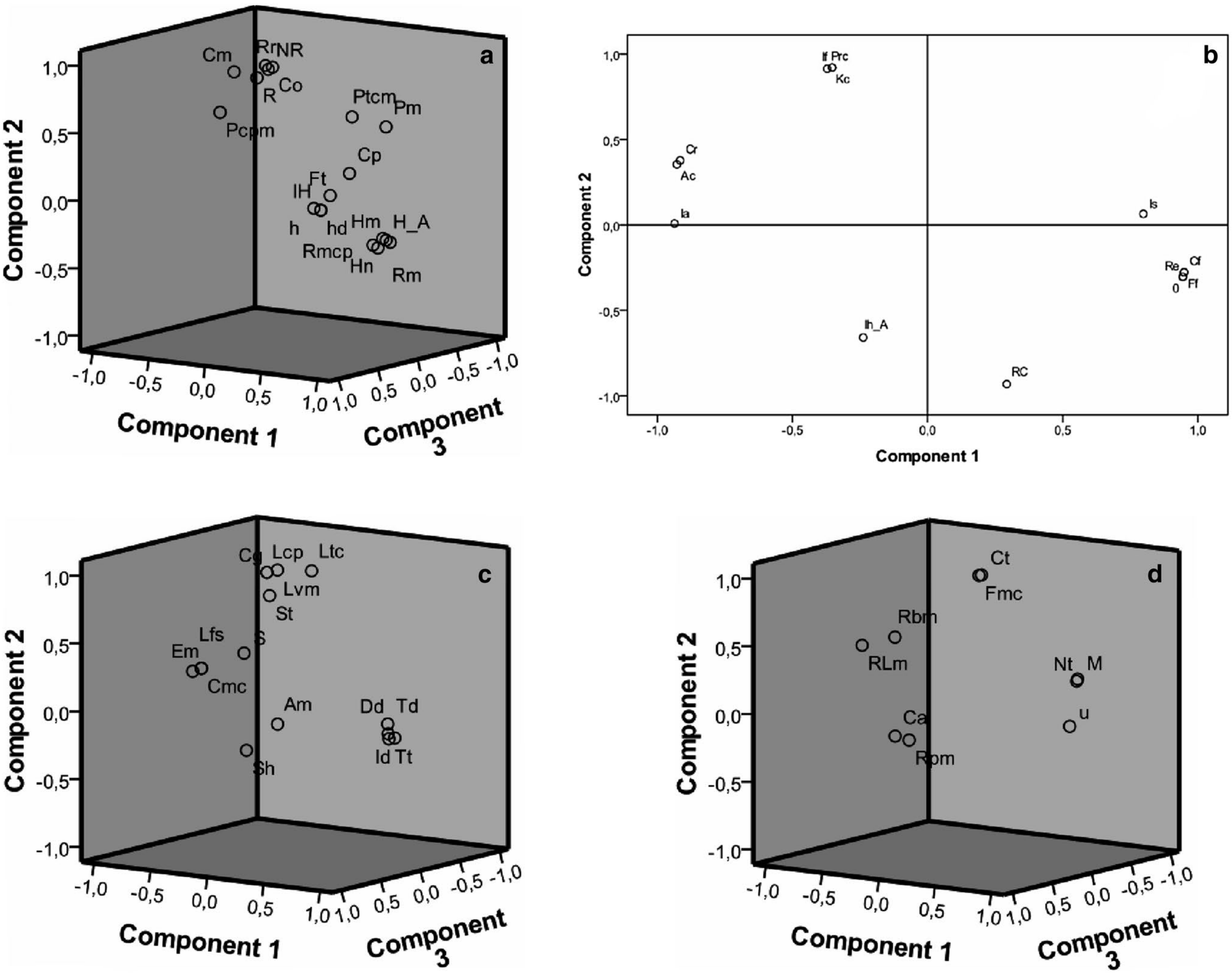

Fig. 5 PC diagrams in rotated space of the morphometric parameters corresponding to the variables **a** gradient and shape of the watershed relief, **b** watershed shape, **c** extension of the drainage network and **d** order and magnitude of the drainage network

and low determination indices (between 0.533 and 0.551). The significance demonstrated low values (between 0.006 and 0.007) and the Durbin–Watson test gave values greater than 1.4, indicating that there were no serious or important autocorrelations, so the variables considered in the model appear to be independent. Better results have been obtained with the gradient and shape of the watershed relief variable, indicating that these morphometric parameters are good predictors of debris volumes. For the shape of the watershed shape variable, the statistical evaluators of the efficiency of the models presented less optimal values, indicating a less reliable variable as a predictor of sediment volumes.

Very good results have been obtained with the extension of the drainage network variable, although slightly less adapted than the gradient and shape of the watershed relief variable, with which these models are considered as quite acceptable predictors. The resulting models with the order and magnitude of the drainage network variable showed very low correlation coefficients and determination indices. With very high significance and Durbin–Watson test values greater than 1.4, the data reveal that the morphometric parameters of this variable cannot be considered as predictors of sediment volumes.

In the results of MLRA-generated β-coefficients between the PC of each one of the morphometric parameters groups and the sediment volume parameters, we observed that for the watershed scale variable, all the predictive models have been presented as acceptable alternatives for estimating the magnitudes of sediment volumes, since the 95% confidence intervals for β occupy ranges or amplitudes greater than zero. As a result, all these predictive models are satisfied with the single PC generated for such variable.

The predictive models, which correspond to the gradient and shape of the watershed relief variable, satisfy only

Table 5 Predictive statistical-mathematical models (equations) of sediment volumes

Hydrological response parameter	Morphometric variable	Predictive statistical-mathematical model of sediment volumes
Sediment volume (event of December 1999) (Vs-Dec1999) (m^3)	Watershed scale	$Y=\beta_0+\beta_1X_1$ Vs-Dec1999 = 1,664,659.595 + 387,055.437(PC1)
	Gradient and shape of the watershed relief	$Y=\beta_0+\beta_2X_2+\beta_3X_3$ Vs-Dec1999 = 1,774,218.744 + (− 456,631.453(PC2)) + (− 361,128.173(PC3))
	Watershed shape	$Y=\beta_0+\beta_1X_1$ Vs-Dec1999 = 1,689,853.701 + 300,943.038(PC1)
	Extension of the drainage network	$Y=\beta_0+\beta_1X_1+\beta_2X_2+\beta_3X_3$ Vs-Dec1999 = 1,710,616.073 + (− 249,259.773(PC1)) + 224,241.079(PC2) + (− 328,038.396(PC3))
Sediment volume prior to the debris flows (Tr = 100 years) ($Vs_{prior\text{-}df}$) (m^3)	Watershed scale	$Y=\beta_0+\beta_1X_1$ $Vs_{prior\text{-}df}$ = 856,136.743 + 212,589.038(PC1)
	Gradient and shape of the watershed relief	$Y=\beta_0+\beta_2X_2+\beta_3X_3$ $Vs_{prior\text{-}df}$ = 914,395.354 + (− 258,457.229(PC2)) + (− 160,091.436(PC3))
	Watershed shape	$Y=\beta_0+\beta_1X_1$ $Vs_{prior\text{-}df}$ = 869,802.192 + 178,301.838(PC1)
	Extension of the drainage network	$Y=\beta_0+\beta_2X_2$ $Vs_{prior\text{-}df}$ = 872,484 + 152,077.774(PC2)
Sediment volume after the debris flows (Tr = 100 years) ($Vs_{after\text{-}df}$) (m^3)	Watershed scale	$Y=\beta_0+\beta_1X_1$ $Vs_{after\text{-}df}$ = 1,011,982.558 + 214,648.581(PC1)
	Gradient and shape of the watershed relief	$Y=\beta_0+\beta_2X_2+\beta_3X_3$ $Vs_{after\text{-}df}$ = 1,073,998.700 + (− 266,846.725(PC2)) + (− 169,819.436(PC3))
	Watershed shape	$Y=\beta_0+\beta_1X_1$ $Vs_{after\text{-}df}$ = 1,025,933.695 + 188,337.200(PC1)
	Extension of the drainage network	$Y=\beta_0+\beta_2X_2$ $Vs_{after\text{-}df}$ = 1,028,949.535 + 155,519.996(PC2)

PCs 2 and 3, reaching 95% confidence intervals for β, but biased towards negative values, whereas PC 1 and 4 have been excluded from the models, since zero is included within their 95% confidence intervals for β. The watershed shape variable, of the two PCs representative of their morphometric parameters, only the first satisfies the predictive models, with 95% confidence intervals for β, which is towards the positive values.

In the predictive models of the extension of the drainage network variable, it is perceived that for the sediment volumes parameter of the December 1999 debris flows event, the three representative PCs of the morphometric parameters satisfy these models, with the intervals of 95% confidence for β of PC 1 and 3 less than zero and that of PC 2 greater than this value. In the case of the sediment volumes before and after the December 1999 debris event, only the PC 2 satisfies the models. Therefore, PCs 1 and 3 have been discarded for the construction of such. For the order and magnitude of the drainage network variable, none of the three PCs representative of their morphometric parameters satisfies their respective predictive models, since the 95% confidence intervals for β in these cases include the zero value in their ranges.

Predictive models of debris volumes

Predictive models with linear equations have been constructed with the PC of each morphometric variable and for each sediment volume parameter (Table 5). The magnitudes of the latter have been estimated, by comparing them later with the magnitudes taken as input data in the analysis statistics, by adjusting the Pearson's correlation coefficients (Table 6).

These models only worked with the watershed scale, gradient and shape of the watershed relief, watershed shape and extension of the drainage network variables. The sediment volumes from December 1999 debris flow event, its best predictive models have been represented by the gradient and shape of the watershed relief and extension of the drainage network variables, while with the watershed scale, watershed shape and order and magnitude of the drainage network variables, their correlation coefficients indicate that these models have not been very efficient as predictors. With the sediment volumes before and after the debris flows event of December 1999, only those generated with morphometric parameters of the gradient and shape of the watershed relief variable functioned as good predictive

Table 6 Sediment volume magnitudes estimated with the predictive models

Watershed	Sediment volume (event of December 1999) (Vs-Dec1999) (m^3)	Sediment volume (event of December 1999) (Vs-Dec1999) (m^3) estimated by the predictive models generated by the MLRA			
		Watershed scale	Gradient and shape of the watershed relief	Watershed shape	Extension of the drainage network
Piedra Azul Creek	2,217,861	1,925,063.29	2,277,070.78	2,159,918.65	2,188,299.54
Osorio Creek	839,182	1,229,814.17	894,098.72	1,457,742.28	911,380.99
Cariaco Creek	1,000,866	1,281,404.69	914,472.71	1,443,841.72	1,380,026.32
San José de Galipán River	1,616,197	1,715,099.69	1,536,783.07	1,631,065.51	1,569,855.09
El Cojo Creek	1,142,693	1,313,750.28	1,620,437.71	1,236,462.07	949,554.75
Camurí Chiquito Creek	1,789,882	1,515,614.55	1,573,113.13	1,282,778.15	1,690,184.48
San Julián Creek	2,636,280	1,969,484.30	2,505,443.51	1,794,523.78	2,285,280.11
Seca Creek	1,616,905	1,134,825.87	1,426,682.20	1,586,751.31	1,310,878.51
Cerro Grande River	1,680,163	2,147,120.38	1,762,363.27	1,750,455.89	2,012,930.76
Uria River	1,396,063	1,637,631.65	1,414,705.43	1,944,049.63	1,719,094.03
Naiguatá River	2,070,029	2,323,234.67	2,114,649.91	2,222,464.94	1,905,491.36
Camurí Grande River	2,225,500	2,038,577.48	2,205,064.76	1,735,883.93	2,308,645.07
Correlation coefficient		0.73	**0.94**	0.58	**0.89**
Watershed	Sediment volume prior to the debris flows (Tr = 100 years) ($Vs_{prior\text{-}df}$) (m^3)	Sediment volume prior to the debris flows (Tr = 100 years) ($Vs_{prior\text{-}df}$) (m^3) estimated by the predictive models generated by the MLRA			
		Watershed scale	Gradient and shape of the watershed relief	Watershed shape	Extension of the drainage network
Piedra Azul Creek	1,313,876.6	999,162.69	1,216,658.95	1,148,304.88	909,752.83
Osorio Creek	484,302.0	617,299.20	444,196.55	732,281.51	709,350.73
Cariaco Creek	598,214.6	645,635.13	450,843.25	724,045.74	699,402.64
San José de Galipán River	949,533.7	883,840.81	794,429.03	834,971.54	1,036,887.86
El Cojo Creek	645,815.8	663,400.85	789,944.06	601,178.07	806,957.72
Camurí Chiquito Creek	790,841.8	774,274.20	802,438.18	628,619.28	867,507.73
San Julián Creek	1,167,764.1	1,023,560.80	1,226,590.56	931,816.81	842,415.62
Seca Creek	701,950.7	565,127.16	716,326.57	808,716.39	705,172.34
Cerro Grande River	726,539.7	1,121,126.88	939,402.05	905,707.60	1,050,305.94
Uria River	594,491.5	841,291.72	778,451.95	1,020,407.44	850,902.72
Naiguatá River	1,171,900.4	1,217,857.13	1,122,092.11	1,185,362.12	1,174,135.18
Camurí Grande River	1,268,855.7	1,061,510.02	1,163,948.49	897,074.04	976,490.02
Correlation coefficient		0.74	**0.90**	0.63	0.59
Watershed	Sediment volume after the debris flows (Tr = 100 years) ($Vs_{after\text{-}df}$) (m^3)	Sediment volume after the debris flows (Tr = 100 years) ($Vs_{after\text{-}df}$) (m^3) estimated by the predictive models generated by the MLRA			
		Watershed scale	Gradient and shape of the watershed relief	Watershed shape	Extension of the drainage network
Piedra Azul Creek	1,450,556.8	1,156,394.13	1,384,269.23	1,320,111.35	1,067,061.93
Osorio Creek	559,328.6	770,831.17	585,678.27	880,672.93	862,123.80
Cariaco Creek	763,351.3	799,441.63	593,040.31	871,973.64	851,950.55
San José de Galipán River	1,105,391.8	1,039,955.02	948,663.16	989,142.67	1,197,074.61
El Cojo Creek	785,742.1	817,379.46	949,333.52	742,190.60	961,940.10
Camurí Chiquito Creek	955,779.3	929,326.94	958,216.14	771,176.28	1,023,860.62
San Julián Creek	1,339,209.2	1,181,028.60	1,406,726.63	1,091,438.68	998,200.57
Seca Creek	924,004.9	718,153.70	869,639.72	961,409.80	857,850.84
Cerro Grande River	855,618.0	1,279,539.90	1,096,573.52	1,063,859.97	1,210,796.41
Uria River	773,861.3	996,993.72	926,735.08	1,185,015.46	1,006,879.77
Naiguatá River	1,379,301.3	1,377,207.26	1,286,902.26	1,359,254.28	1,337,428.47
Camurí Grande River	1,393,452.4	1,219,345.48	1,331,070.34	1,054,740.49	1,135,309.69
Correlation coefficient		0.73	**0.90**	0.65	0.59

Bold values represent the best correlation coefficients obtained between the initial sediment volumes estimated by Córdova and González (2003) and those estimated by the predictive models obtained in this research models. The rest of the morphometric variables obtained very poor quality adjustments, as evidenced by the low correlation coefficients.

Conclusions

The sediment volumes, which have been previously estimated and taken as input in this study, reveal important magnitudes in the yield, transport and deposition of sediments, related to the occurrence of extreme rainfall events, clearly demonstrating the hazard. It is obvious that flash floods represent these hydro-geomorphological systems.

The LCA revealed good correlations between the sediment volumes and most of the morphometric parameters corresponding to the watershed scale variable, as well as some parameters of the gradient and shape of the watershed relief variable.

The PCA has reduced the dimensionality of the morphometric parameters groups, defining as new variables the components or factorials created for each group or initial morphometric variable.

The MLRA with PC of the morphometric variables gave very good correlation and determination indices between the sediment volumes and the PC's of the gradient and shape of the watershed relief variable, as well as good indices with the PC's of the extension of the drainage network and watershed scale variables.

For each sediment volumes parameter considered in this study, predictive models of such hydrological responses have been obtained from the MLRA. Each model responds to the PC's with a set of morphometric parameters grouped in morphometric variables. In this way, the estimations of magnitudes of the sediment volumes with the predictive models generated in this research, and compared with the magnitudes taken as input data, revealed that the most suitable models are those corresponding to the gradient and shape of the watershed relief variable.

Among some interesting aspects to develop in future research studies, related to factors and/or elements of the physical environment as predictors of the occurrence of debris flow events, we expect to: (a) analyze the particular relations morphometric parameters of the drainage networks with each of the lithological outcrops and each vegetation formation. This will support the understanding of the weight of each type of rock and vegetation in sediments production and, in its differential contribution to the generation of debris flows; (b) to study in detail and in a comparative way the depth of the alteration profiles, the volumes of regolith and its mineralogy, developed on each type of rock, to identify lithologies that contribute most in the activation of debris flows; and (c) analyze the density and depth of the root system of each vegetation formation in the soils, in terms of the relative stability they offer to the materials of the slopes, considering the topographic slope as a conditioning element.

Acknowledgements The authors are very grateful to the Fondo para el Desarrollo de la Investigación (FONDEIN) of the Universidad Pedagógica Experimental Libertador – Instituto Pedagógico de Caracas (UPEL-IPC) (Caracas, Venezuela), for the financial support of the research project from which this paper has been derived. We would like also to thank the editorial handling, Rachid Seqqat and two anonymous reviewers for the significant improvement of an earlier version of this article.

References

Amend S (1991) El Ávila National Park (national parks and environmental conservation N° 2) (Parque Nacional El Ávila (Parques Nacionales y Conservación Ambiental N° 2)). Stephan y Thora Amend, Caracas

Artigas J, Córdova J (2010) Estimation of volumes and peaks of debris flows and sediment yield in Vargas State watersheds (Estimación de volúmenes y picos de aludes torrenciales y producción de sedimentos en cuencas del estado Vargas). In: López J (ed) Lecciones aprendidas del desastre de Vargas: aportes científico-tecnológicos y experiencias nacionales en el campo de la prevención y mitigación de riesgos. Instituto de Mecánica de Fluidos, Facultad de Ingeniería, Universidad Central de Venezuela, Caracas, pp 239–257

Artigas J, López J, Córdova J (2004) Sediment yield in the watersheds of the southern slopes of El Ávila National Park (Producción de sedimentos en las cuencas de la vertiente sur del Parque Nacional El Ávila). Dissertation, Universidad Central de Venezuela

Artigas J, López JL, Córdova JR (2006) Methodology to estimate the total sediment transport in mountainous river basins. Revista Técnica de la Facultad de Ingeniería 29(3):221–234

Ballesteros-Cánovas JA, Czajka B, Janecka K, Lempa M, Kaczka RJ, Stoffel M (2015) Flash floods in the Tatra Mountain streams: frequency and triggers. Sci Total Environ 511:639–648

Bel C, Liébault F, Navratil O, Eckert N, Bellot H, Fontaine F, Ligle D (2017) Rainfall control of debris-flow triggering in the Réal Torrent, Southern French Prealps. Geomorphology 291:17–32. https://doi.org/10.1016/j.geomorph.2016.04.004

Bremer M, Sass O (2012) Combining airborne and terrestrial laser scanning for quantifying erosion and deposition by a debris flow event. Geomorphology 138:49–60. https://doi.org/10.1016/j.geomorph.2011.08.024

Centro de Procesamiento Digital de Imágenes (1999) IKONOS pancromática, resolución espacial 1 metro. Baruta

Chen HX, Zhang S, Peng M, Zhang LM (2016) A physically-based multi-hazard risk assessment platform for regional rainfall-induced slope failures and debris flows. Eng Geol 203:15–29. https://doi.org/10.1016/j.enggeo.2015.12.009

Córdova J, González M (2003) Estimation of the volumes and maximum discharges produced by the debris flows occurred in December 1999 in the watersheds of the Central Coast of Vargas State, Venezuela (Estimación de los volúmenes y caudales máximos que produjeron los aludes torrenciales ocurridos en Diciembre de 1999 en cuencas del Litoral Central del estado Vargas, Venezuela). Acta Cient Venez 54(1):33–48

Costa JE (1984) Physical geomorphology of debris flows. In: Costa JE, Fleisher PJ (eds) Developments and applications of geomorphology. Springer, Berlin, pp 268–317

Costa JE (1988) Rheologic, geomorphic, and sedimentologic differentiation of water floods, hyperconcentrated flows, and debris flows. In: Baker VR, Kochel RC, Patton PC (eds) Flood Geomorphology. Wiley, New York, pp 113–122

Coussot P, Meunier M (1996) Recognition, classification and mechanical description of debris flows. Earth Sci Rev 40(3):209–227

De Martonne E (1909) Treatise of physical geography (Traité de géographie physique). A. Colin, Paris

Destro E, Marra F, Nikolopoulos E, Zoccatelli E, Creutin JD, Borga M (2017) Spatial estimation of debris flows-triggering rainfall and its dependence on rainfall return period. Geomorphology 278:269–279. https://doi.org/10.1016/j.geomorph.2016.11.019

Dietrich A, Krautblatter M (2017) Evidence for enhanced debris-flow activity in the Northern Calcareous Alps since the 1980s (Plansee, Austria). Geomorphology 287:144–158. https://doi.org/10.1016/j.geomorph.2016.01.013

Dirección de Cartografía Nacional (1958) Hojas II-8, III-8, IV-8, I-9, II-9, III-9, IV-9, I-10, II-10, III-10, IV-10, I-11, II-11, III-11, IV-11, I-12, II-12, III-12, IV-12, I-13, II-13, III-13 y IV-13 [Planos topográficos a escala 1:5.000, Proyecto BITUCOTEX]. Caracas

Dirección de Cartografía Nacional (1979) Hoja 6847-IV-SO 23 de Enero; Hoja 6847-I-SO Curupao; Hoja 6847-IV-NE El Caribe; Hoja 6847-IV-SE Los Chorros; Hoja 6847-IV-NO Maiquetía; y Hoja 6847-I-NO Naiguatá [Cartas topográficas a escala 1:25.000]. Caracas

Fan L, Lehmann P, McArdell B, Or D (2017) Linking rainfall-induced landslides with debris flows runout patterns towards catchment scale hazard assessment. Geomorphology 280:1–15. https://doi.org/10.1016/j.geomorph.2016.10.007

Faniran A (1968) The index of drainage intensity—a provisional new drainage factor. Aust J Sci 31(9):328–330

García-Martínez R, Lopez JL (2005) Debris flows on December 1999 in Venezuela. In: Jakob M, Hungr O (eds) Chapter 20 of debris-flow hazards and related phenomena. Springer, Berlin

Gardiner V (1981) Drainage basin morphometry. In: Goudie A (ed) Geomorphological techniques. George Allen & Unwin, London, pp 47–55

Giannecchini R, Galanti Y, D'Amato Avanzi G, Barsanti M (2016) Probabilistic rainfall thresholds for triggering debris flows in a human-modified landscape. Geomorphology 257:94–107. https://doi.org/10.1016/j.geomorph.2015.12.012

Gobernación del Distrito Federal (1984) Hojas B-42, C-42, D-42, E-42, B-43, C-43, D-43, E-43, B-44, C-44, D-44, B-45, B-46, B-47, B-48 y B-49 [Planos topográficos a escala 1:5.000]. Caracas

Gravelius H (1914) River science (Flusskunde). Goschen Verlagshandlug Berlin. In: Zavoianu I (1985) (ed) Morphometry of drainage basins. Elsevier, Amsterdam

Hack J (1957) Studies of longitudinal stream profiles in Virginia and Maryland. U. S. Geological Survey Prof. Paper 294-B

Hadley RF, Schumm SA (1961) Sediment sources and drainage basin characteristics in upper Cheyenne River basin. US Geological Survey Water-Supply Paper 1531:198

Henao J (1998) Introduction to watershed management (Introducción al manejo de cuencas hidrográficas). Universidad Santo Tomás, Santafé de Bogotá

Hernández E (2006) Mud flows and debris flows during the storms of December 15 and 16, 1999 in the Vargas State, Venezuela (Flujos de barros y escombros durante las tormentas de los días 15 y 16 de diciembre de 1999 en el edo. Vargas, Venezuela). In: López J, García R (eds) Los aludes torrenciales de Diciembre 1999 en Venezuela. Instituto de Mecánica de Fluidos, Facultad de Ingeniería, Universidad Central de Venezuela, Caracas, pp 443–453

Horton R (1932) Drainage basin characteristics. Trans Am Geophys Union 13:350–361. https://doi.org/10.1029/TR013i001p00350

Horton R (1945) Erosional development of streams and their drainage basins: hydrophysical approach to quantitative morphology. Geol Soc Am Bull 56:275–370. https://doi.org/10.1130/0016-7606(1945)56%5b275:EDOSAT%5d2.0.CO;2

Hotelling H (1933) Analysis of a complex of statistical variables into principal components. J Educ Psychol 24:417–441/498–520

Huber O, Alarcón C (1988) Vegetation map of Venezuela (Mapa de la vegetación de Venezuela) [Mapa a escala 1:2.000.000]. Caracas

Instituto Geográfico de Venezuela Simón Bolívar (2003) Caracas and surroundings (Caracas y alrededores) (Mapa Especial) [Mapa a escala 1:100.000]. Caracas

Iverson RM (1997) The physics of debris flows. Rev Geophys 35(3):245–296

Jakob M, Hungr O, Jakob DM (2005) Debris-flow hazards and related phenomena, vol 739. Springer, Berlin

Langbein W (1947) Topographic characteristics of drainage basins. U. S. Geological Survey Water Supply Paper 968C:125-157

Larsen MC, Conde MTV, Clark RA (2001a) Landslide hazards associated with flash-floods, with examples from the December 1999 disaster in Venezuela. In: Gruntfest E, Handmer J (eds) Coping with flash floods. Springer, Dordrecht, pp 259–275

Larsen MC, Wieczorek GF, Eaton LS, Morgan BA, Torres-Sierra H (2001b) Venezuelan debris flow and flash flood disaster of 1999 studied. EOS Trans Am Geophys Union 82(47):572–573

Legorreta Paulín G, Bursik M, Zamorano Orozco JJ, Lugo Hubp J, Martínez-Hackert B, Bajo Sánchez JV (2017) Estimation of the deposit volumes linked to landslides through landforms, on the SW flank of the Pico de Orizaba volcano, Puebla-Veracruz (Estimación del volumen de los depósitos asociados a deslizamientos a través de geoformas, en el flanco SW del volcán Pico de Orizaba, Puebla-Veracruz). Investig Geográf 92:1–13. https://doi.org/10.14350/rig.51113

López J, Pérez D, García R, Shucheng Z (2006) Hydro-geomorphological assessment of the debris flows of December 1999 in Venezuela (Evaluación hidro-geomorfológica de los aludes torrenciales de diciembre 1999 en Venezuela). In: López J, García R (eds) los aludes torrenciales de diciembre 1999 en Venezuela. Instituto de Mecánica de Fluidos, Facultad de Ingeniería, Universidad Central de Venezuela, Caracas, pp 41–57

Ma Ch, Wang Y, Hu K, Du C, Yang W (2017) Rainfall intensity–duration threshold and erosion competence of debris flows in four areas affected by the 2008Wenchuan earthquake. Geomorphology 282:85–95. https://doi.org/10.1016/j.geomorph.2017.01.012

Marra F, Nikolopoulos EI, Creutin JD, Borga M (2016) Space–time organization of debris flows-triggering rainfall and its effect on the identification of the rainfall threshold relationship. J Hydrol 541:246–255. https://doi.org/10.1016/j.jhydrol.2015.10.010

Martha T, Reddy P, Bhatt C, Raj K, Nalini J, Padmanabha E, Narender B, Kumar K, Muralikrishnan S, Rao G, Diwakar P, Dadhwal V (2017) Debris volume estimation and monitoring of Phuktal river landslide-dammed lake in the Zanskar Himalayas, India using Cartosat-2 images. Landslides 14(1):373–383. https://doi.org/10.1007/s10346-016-0749-8

Martin Y, Johnson E, Chaikina O (2017) Gully recharge rates and debris flows: a combined numerical modelling and field-based investigation, Haida Gwaii, British Columbia. Geomorphology 278:252–268

Martínez E (2010) Methods of hydrological and hydraulic calculations of the debris flows in Vargas of 1999 from field observation (Métodos de cálculos hidrológicos e hidráulicos de los flujos en Vargas de 1999 a partir de la observación de campo). In: López J (ed) Lecciones aprendidas del desastre de Vargas: aportes científico-tecnológicos y experiencias nacionales en el campo de la prevención y mitigación de riesgos. Instituto de Mecánica de Fluidos, Facultad de Ingeniería, Universidad Central de Venezuela, Caracas, pp 345–355

Melton M (1957) An analysis of the relations among elements of climate, surface properties, and geomorphology (Project NR 389-042, Tech. Rept. 11). Columbia University, Dept. of Geology, ONR, Geography Branch, New York

Melton M (1958) Geometric properties of mature drainage systems and their representation in an E_4 phase space. J Geol 66:35–54. https://doi.org/10.1086/626481

Melton M (1965) The geomorphic and paleoclimatic significance of alluvial deposits in southern Arizona. J Geol 73:1–38. https://doi.org/10.1086/627044

Miller V (1953) A quantitative geomorphic study of drainage basin characteristics in the Clinch Mountain area, Virginia and Tennessee (Project NR 389-042, Tech. Rept. 3). Columbia University, Dept. of Geology, ONR, Geography Branch, New York

Morisawa M (1985) Rivers: form and process. Longman, London

Mueller J (1968) An introduction to the hydraulic and topographic sinuosity indexes. Ann Assoc Am Geogr 58:371–385. https://doi.org/10.1111/j.1467-8306.1968.tb00650.x

Nadim F, Kjekstad O, Peduzzi P, Herold C, Jaedicke C (2006) Global landslide and avalanche hotspots. Landslides 3(2):159–173

Palau RM, Hürlimann M, Pinyol J, Moya J, Victoriano A, Génova M, Puig-Polo C (2017) Recent debris flows in the Portainé catchment (Eastern Pyrenees, Spain): analysis of monitoring and field data focussing on the 2015 event. Landslides 14(3):1161–1170

Pearson K (1901) On lines and planes of closest fit to systems of points in space. Phil Mag 2:559–572

Pérez FL (2001) Matrix granulometry of catastrophic debris flows (December 1999) in central coastal Venezuela. CATENA 45(3):163–183

Pike RJ, Wilson SE (1971) Elevation- relief ratio hypsometric integral and geomorphic area-altitude analysis. Geol Soc Am Bull 82:1079–1084. https://doi.org/10.1130/0016-7606(1971)82%5b1079:ERHIAG%5d2.0.CO;2

Potter W (1953) Rainfall and topographic factor that affect run-off. Trans Am Geophys Union 34:67–73. https://doi.org/10.1029/TR034i001p00067

Roche M (1963) Hydrology of surface. Gauthier-Villars, Paris

Santi PM, Hewitt K, VanDine DF, Cruz EB (2011) Debris-flow impact, vulnerability, and response. Nat Hazards 56(1):371–402

Schumm S (1956) Evolution of drainage basins and slopes in badlands at Perth Amboy, New Jersey. Bull Geol Soc Am 67:597–646. https://doi.org/10.1130/0016-7606(1956)67%5b597:EODSAS%5d2.0.CO;2

Schumm S (1963) Sinuosity of alluvial rivers on the great plains. Geol Soc Am Bull 74:1089–1100. https://doi.org/10.1130/0016-7606(1963)74%5b1089:SOAROT%5d2.0.CO;2

Schumm S (1977) The fluvial system. Wiley, New York

Servicio Autónomo de Geografía y Cartografía Nacional (1995) Hoja 6847-IV-NE Caraballeda; Hoja 6847-IV-SO Caracas; Hoja 6847-I-SO Curupao; Hoja 6847-IV-NO La Guaira; Hoja 6847-IV-SE Los Chorros; y Hoja 6847-I-NO Naiguatá [Ortofotomapas a escala 1:25.000]. Caracas

Seyhan E (1977) The watershed as an hydrologic unit. Geografisch Inst. der Rijksuniv, Utrecht

Shreve R (1974) Variations of mainstream length with basin area in river networks. Water Resour Res 10(6):1167–1177. https://doi.org/10.1029/WR010i006p01167

Smith K (1950) Standards for grading texture of erosional topography. Am J Sci 248:655–668. https://doi.org/10.2475/ajs.248.9.655

Sreedevi PD, Subrahmanyam K, Ahmed S (2005) The significance of morphometric analysis for obtaining groundwater potential zones in a structurally controlled terrain. Environ Geol 47(3):412–420. https://doi.org/10.1007/s00254-004-1166-1

Steyermark J, Huber O (1978) Flora of Ávila: flora and vegetation of the mountains of Ávila, La Silla and Naiguatá (Flora del Ávila: flora y vegetación de las montañas del Ávila, de la Silla y del Naiguatá). Sociedad Venezolana de Ciencias Naturales, Völlmer Foundation, Ministerio del Ambiente y de los Recursos Naturales Renovables, Caracas

Strahler A (1952) Dynamic basis of geomorphology. Bull Geol Soc Am 63:923–938. https://doi.org/10.1130/0016-7606(1952)63%5b923:DBOG%5d2.0.CO;2

Strahler A (1957) Quantitative analysis applied of watershed geomorphology. Trans Am Geophys Union 38:913–920. https://doi.org/10.1029/TR038i006p00913

Strahler A (1964) Quantitative geology of drainage basins and channel networks. In: Chow V (ed) Handbook of applied hydrology. McGraw-Hill Book Co., New York, pp 39–76

Tichavský R, Šilhán K (2015) Dendrogeomorphic approaches for identifying the probable occurrence of debris flows and related torrential processes in steep headwater catchments: the Hrubý Jeseník Mountains, Czech Republic. Geomorphology 246:445–457

Tiranti D, Cavalli M, Crema S, Zerbato M, Graziadei M, Barbero S, Cremonini R, Silvestro C, Bodrato G, Tresso F (2016) Semi-quantitative method for the assessment of debris supply from slopes to river in ungauged catchments. Sci Total Environ 554–555:337–348

Urbani F (1999) Review of the igneous and metamorphic rock units of the Coastal Mountain Range, Venezuela (Revisión de las unidades de rocas ígneas y metamórficas de la Cordillera de la Costa, Venezuela). GEOS (Caracas, Escuela de Geologìa Y Minas, Universidad Central de Venezuela) 33:1–170

Urbani F (2000) Geological considerations of the Vargas State disaster of December 1999 (Consideraciones geológicas de la catástrofe del estado Vargas de diciembre de 1999). In: Memorias del XVI Seminario Venezolano de Geotecnia: calamidades geotécnicas urbanas con visión al siglo XXI, la experiencia para proyectos del futuro. Sociedad Venezolana de Geotecnia, Caracas, pp 179–193

Urbani F (2002a) The Miguelena river of Camurí Grande, Vargas State: a window to the geology of the Coastal Mountain Range—excursion guide (Geological Excursions N° 02-1) (El río Miguelena de Camurí Grande, estado Vargas: una ventana a la geología de la Cordillera de la Costa—guía de excursión (Excursiones Geológicas N° 02-1)). Sociedad Venezolana de Geólogos, Comité Metropolitano de Excursiones, Caracas

Urbani F (2002b) Geology of the highway area and old road Caracas—La Guaira, Capital District and Vargas State: excursion guide (Geología del área de la autopista y carretera vieja Caracas—La Guaira, Distrito Capital y estado Vargas: guía de excursión). Geos (Caracas, Escuela de Geologìa Y Minas, Universidad Central de Venezuela) 35:1–75

Urbani F (2002c) Geology of the Vargas State and the igneous-metamorphic units of the Coastal Mountain Range (Geología del estado Vargas y las unidades ígneo-metamórficas de la Cordillera de la Costa). In: Memorias del III Coloquio sobre Microzonificación Sísmica y III Jornadas de Sismología Histórica (Colección Serie Técnica Nº 2). Fundación Venezolana de Investigaciones Sismológicas, Caracas, pp 236–240

Urbani F (2002d) Nomenclature of the igneous and metamorphic rock units of the Coastal Mountain Range, Venezuela (Nomenclatura de las unidades de rocas ígneas y metamórficas de la Cordillera de la Costa, Venezuela). Geos (Caracas, Escuela de Geologìa Y Minas, Universidad Central de Venezuela) 35:1–83

Urbani F, Rodríguez J, Barboza L, Rodríguez S, Cano V, Melo L, Castillo A, Suárez J, Vivas V, Fournier H (2006) Geology of the Vargas State, Venezuela (Geología del estado Vargas, Venezuela). In: López J, García R (eds) Los aludes torrenciales de Diciembre 1999 en Venezuela. Instituto de Mecánica de Fluidos, Facultad de Ingeniería, Universidad Central de Venezuela, Caracas, pp 133–156

Vallance JW, Scott KM (1997) The Osceola Mudflow from Mount Rainier: Sedimentology and hazard implications of a huge clay-rich debris flow. Geol Soc Am Bull 109(2):143–163. https://doi.org/10.1130/0016-7606(1997)109<0143:TOMFMR>2.3.CO;2

van Steijn H (1996) Debris-flow magnitude—frequency relationships for mountainous regions of Central and Northwest Europe. Geomorphology 15(3–4):259–273. https://doi.org/10.1016/0169-555X(95)00074-F

Vareschi V (1992) Ecology of the tropical vegetation: with special attention to research in Venezuela (Ecología de la vegetación tropical: con especial atención a investigaciones en Venezuela). Sociedad Venezolana de Ciencias Naturales, Caracas

Wei Z, Shang Y, Zhao Y, Pan P, Jiang Y (2017) Rainfall threshold for initiation of channelized debris flows in a small catchment based on in-site measurement. Eng Geol 217:23–34. https://doi.org/10.1016/j.enggeo.2016.12.003